Quantum Oscillations in Antiferromagnetic Conductors with Small Carrier Pockets

Revaz Ramazashvili

Laboratoire de Physique Théorique—IRSAMC, CNRS and Université de Toulouse, UPS, F-31062 Toulouse, France

(Received 1 June 2010; published 16 November 2010)

I study magnetic quantum oscillations in antiferromagnetic conductors with small carrier pockets and show that combining the oscillation data with symmetry arguments and with the knowledge of the possible positions of the band extrema may allow us to greatly constrain or even uniquely determine the location of a detected carrier pocket in the Brillouin zone.

DOI: 10.1103/PhysRevLett.105.216404 PACS numbers: 71.18.+y, 74.72.−h, 75.50.Ee

For over 50 years, magnetic quantum oscillations have been used as a direct and precise probe of the Fermi surface physics in metals [1]. The scope of the quantum oscillation experiments has been ever expanding to new materials such as layered and chain compounds, magnetically ordered metals, and superconductors.

Recently, quantum oscillations were successfully observed in $YBa_2Cu_3O_{6+x}$ (YBCO) cuprate superconductors [2–7], prominent members of the family of doped antiferromagnetic insulators. In the underdoped region of the phase diagram, well-defined charged quasiparticles with a small-pocket Fermi surface were the key findings, whose further systematic study has only begun.

The small size of the carrier pockets points to an electron ordering and a concomitant Fermi surface reconnection; several types of order, including the *ortho*-II chain structure [8], stripelike spin density wave [9,10], and field-induced antiferromagnetism [11] were evoked to account for the observed area of the pockets. Distinguishing between these possibilities purely theoretically appears problematic: to reach agreement with quantum oscillation data, band structure calculations often require rigid shifts in the relative positions of the bands [8] and fitting renormalization factors [9]. These *ad hoc* adjustments may become substantial for small carrier pockets, let alone the unidentified nature of the electron order likely affecting the band structure in an unknown way. Given that probing the YBCO Fermi surface by angle-resolved photoemission remains a challenge, it is desirable to distinguish between the various ordering scenarios by means of only the quantum oscillations. This invites a question that is relevant far beyond the physics of the cuprates: how do various types of order manifest themselves in the quantum oscillations, and how much can one possibly learn about a given type of order from a quantum oscillation measurement alone?

An important step in this direction has been undertaken recently by Kabanov and Alexandrov [12], who studied the effect of the Zeeman splitting on the quantum oscillations in a weakly doped two-dimensional insulator of square symmetry with the Néel antiferromagnetic order. The authors studied the reduction factor R_s, modulating the nth harmonic amplitude due to interference of the contributions from the two Zeeman-split branches of the spectrum [1],

$$R_s = \cos\left[\pi n \frac{\delta\mathcal{E}}{\Omega_0}\right], \tag{1}$$

where $\delta\mathcal{E}$ is the Zeeman splitting of the Landau levels and Ω_0 the cyclotron energy. They showed that the R_s depends on the orientation of the field relative not only to the conducting plane, but also to the staggered magnetization (Fig. 1). Moreover, in a spin-flop configuration, where the staggered magnetization reorients itself transversely to the field, the Landau levels undergo *no* Zeeman splitting [13,14], and the R_s equals unity as long as the field $\mathbf{H}$ exceeds the spin-flop threshold [12]. This behavior is in stark contrast to that of a two-dimensional paramagnetic conductor with the isotropic Zeeman term $\mathcal{H}_Z = -\frac{1}{2}\mu_B g(\mathbf{H}\cdot\boldsymbol{\sigma})$, where the R_s reads

$$R_s = \cos\left[\pi n \frac{g\mu_B mc}{\hbar e\cos\theta}\right], \tag{2}$$

with $\mu_B = \frac{1}{2}\frac{|e|\hbar}{m_e c}$ being the Bohr magneton, m the cyclotron mass, and θ the inclination angle, as sketched in Fig. 1: regardless of the value of g, the R_s in Eq. (2) has infinitely many "spin zeros" as a function of θ.

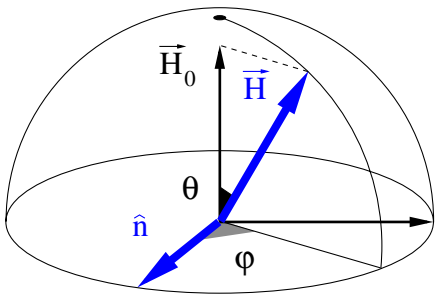

FIG. 1 (color online). The staggered magnetization $\mathbf{n}$, pointing along the conducting plane, the magnetic field $\mathbf{H}$ and its normal component $\mathbf{H}_0$ with respect to the conducting plane. The orientation of the field is defined by the inclination angle θ and by the azimuthal angle φ, as shown in the figure.

The peculiar behavior of the R_s, predicted in Ref. [12], stems from the anisotropic spin-orbit character of the Zeeman coupling $\mathcal{H}_Z$ in an antiferromagnet [15–17]. The energy scale E_{SO} of the relativistic spin-orbit coupling tends to be negligible compared with the antiferromagnetic gap Δ in the electron spectrum. Therefore, in the wide range of magnetic fields $E_{SO} \ll \langle \mathcal{H}_Z \rangle \ll \Delta$ considered hereafter, the Zeeman term is sensitive to the orientation of the field relative to the staggered magnetization, but not to the crystal axes. Hence, in this range of fields, the gyromagnetic factor g in the Zeeman term turns into a tensor with two distinct eigenvalues, $g_\parallel$ and $g_\perp$, for the longitudinal ($\mathbf{H}_\parallel$) and the transverse ($\mathbf{H}_\perp$) components of the magnetic field $\mathbf{H}$ with respect to the staggered magnetization. The $g_\parallel$ is constant up to small relativistic corrections. By contrast, in d dimensions, the $g_\perp$ must vanish on a $(d-1)$-dimensional manifold $\{\mathbf{p}^*\}$ in the Brillouin zone, due to a conspiracy of the crystal symmetry with that of the antiferromagnetic order [16,17]. Thus, the $g_\perp$ must depend substantially on the quasiparticle momentum $\mathbf{p}$:

$$\mathcal{H}_Z = -\tfrac{1}{2}\mu_B[g_\parallel(\mathbf{H}_\parallel \cdot \boldsymbol{\sigma}) + g_\perp(\mathbf{p})(\mathbf{H}_\perp \cdot \boldsymbol{\sigma})]. \quad (3)$$

Whenever a small carrier pocket is centered within the $\{\mathbf{p}^*\}$, the Zeeman splitting in a purely transverse field vanishes [12–14], leading to a peculiar dependence of the R_s on the field direction [12]. No spin zeros appear beyond the spin-flop threshold, and such a behavior of the R_s may serve as a signature of antiferromagnetic order.

A number of new developments suggest that the antiferromagnetism in the underdoped YBCO may be weakly incommensurate rather than commensurate, thus calling for an extension of the above results. Recent neutron scattering data [18] have shown evidence of incommensurate antiferromagnetism, induced by a magnetic field in the underdoped $YBa_2Cu_3O_{6.45}$ of very close composition to the samples of Refs. [2–7]. At the same time, a weakly incommensurate stripelike spin density wave with an ordering wave vector $\mathbf{Q} = (\frac{\pi}{a}[1 - \frac{1}{2N}], \frac{\pi}{a})$, with an integer N (a being the lattice spacing), was found to yield [9,10], in a broad parameter range, small electron pockets, consistent not only with the quantum oscillation data [2–7], but also with the observed negative low-temperature Hall coefficient [19].

How could such a weakly incommensurate antiferromagnetism manifest itself in quantum oscillations? The answer depends on the location of the carrier pocket in the Brillouin zone. Pockets, centered within the $\{\mathbf{p}^*\}$, were described above. Weak incommensurability opens a new possibility: pockets, centered outside the $\{\mathbf{p}^*\}$.

For $\mathbf{Q} = (\frac{3}{4}\frac{\pi}{a}, \frac{\pi}{a})$ and generic values of the density wave parameters, Ref. [9] found such pockets, centered at the points B in Fig. 2(a), while Ref. [10] found analogous pockets for $\mathbf{Q} = (\frac{7}{8}\frac{\pi}{a}, \frac{\pi}{a})$. These pockets are about $\frac{\pi}{2a}$ away from the nearest point S, where the line $g_\perp(\mathbf{p}) = 0$ is pinned by symmetry. In the simplest case, the line

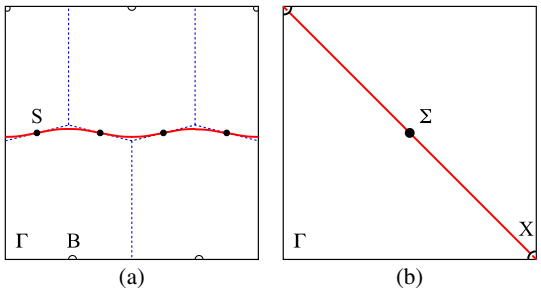

FIG. 2 (color online). (a) The first quadrant of the paramagnetic Brillouin zone of a $\mathbf{Q} = (\frac{3}{4}\frac{\pi}{a}, \frac{\pi}{a})$ antiferromagnet [9]. The dashed (blue) lines denote the antiferromagnetic Brillouin zone boundaries. The thick (red) curve shows a typical line, where $g_\perp(\mathbf{p}) = 0$; this line is pinned by symmetry at the points S at the momenta $\mathbf{p}^* = (\frac{\pi}{8a}[2n+1], \frac{\pi}{2a}[2l+1])$. The band extrema were found [9] at the points B, shown by the open circles, and, in a narrower parameter range, at the points S, shown by dark circles. (b) The same as (a), but for a $\mathbf{Q} = (\frac{\pi}{a}, \frac{\pi}{a})$ Néel antiferromagnet on a lattice of square symmetry. The thick (red) line shows the antiferromagnetic Brillouin zone boundary, where $g_\perp(\mathbf{p}) = 0$. The band extrema were found at the points Σ (black circles) and X (open circles).

$g_\perp(\mathbf{p}) = 0$ is singly connected and pinned at the points S; $g_\perp(\mathbf{p})$ is suppressed only within momentum deviations $|\delta p| \lesssim \xi^{-1} \ll \frac{\pi}{2a}$ from this line [17]. In such a case, the g tensor at the B pockets is isotropic up to vanishingly small corrections of the order of $(a/\xi)^2 \ll 1$, which can be read off from Eq. (11) of Ref. [17] for the $\mathbf{Q} = (\frac{\pi}{a}, \frac{\pi}{a})$ Néel order.

However, a very recent study [20] found the $g_\perp(\mathbf{p}) = 0$ line numerically for a $\mathbf{Q} = (\frac{3}{4}\frac{\pi}{a}, \frac{\pi}{a})$ spin density wave, and discovered that this line may be multiply connected, with components disconnected from symmetry-enforced degeneracy points. Some of these components were found to pass close to the B points. In such cases, the $g_\perp(\mathbf{p})$ for the B pockets is nonzero yet reduced, and thus the g tensor is strongly anisotropic [20]. By contrast with the pockets, centered on the line $g_\perp(\mathbf{p}) = 0$, the Zeeman splitting of the B-pocket Landau levels does *not* vanish, and the spin zeros do appear even in the spin-flop configuration, albeit at greater inclination angles θ.

Do the above observations open any diagnostic opportunities? Of course, spin zeros are no proof of antiferromagnetism. However, having experimental knowledge of the presence and periodicity of the antiferromagnetism in the sample greatly restricts the allowed possibilities: for instance, in $\mathbf{Q} = (\frac{3}{4}\frac{\pi}{a}, \frac{\pi}{a})$ and $\mathbf{Q} = (\frac{7}{8}\frac{\pi}{a}, \frac{\pi}{a})$ spin density wave states, the B points in Fig. 2(a) were the *only* band extrema outside the $\{\mathbf{p}^*\}$, found by Refs. [9,10] for generic parameter values. Thus, observation of spin zeros in such an antiferromagnet constrains the detected carrier pocket uniquely to the center point B of the magnetic Brillouin zone.

By contrast, in a $\mathbf{Q} = (\frac{\pi}{a}, \frac{\pi}{a})$ antiferromagnet, in the relevant parameter range the calculated band minima

were found *only* on the magnetic Brillouin zone boundary [11], where $g_\perp(\mathbf{p}) = 0$. For such carrier pockets, no spin zeros appear in a purely transverse field; thus, observation of spin zeros is essentially incompatible with $\mathbf{Q} = (\frac{\pi}{a}, \frac{\pi}{a})$ Néel antiferromagnetism.

The experiments have not yet reached a consensus. Measurements of the underdoped $YBa_2Cu_3O_{6.54}$ have found no spin zeros within the expected angular range [21]. By contrast, Ref. [22] studied the underdoped $YBa_2Cu_3O_{6.59}$ and did find spin zeros, consistent with the isotropic g tensor, within the range of Ref. [21].

While settling this disagreement is beyond the scope of the present work, eventually finding *no* spin zeros at all would be consistent with antiferromagnetism and the pockets centered within the $\{\mathbf{p}^*\}$. By contrast, between the $\mathbf{Q} = (\frac{\pi}{a}, \frac{\pi}{a})$ and $\mathbf{Q} = (\frac{\pi}{a}[1 - \frac{1}{2N}], \frac{\pi}{a})$ spin density waves, detecting spin zeros would be consistent only with the latter periodicity and with the detected pockets centered uniquely at the B points in Fig. 2(a).

I will now demonstrate the symmetry underpinnings of the above results [17]. In a $\mathbf{Q} = (\frac{\pi}{a}[1 - \frac{1}{2N}], \frac{\pi}{a})$ spin density wave state with an integer N and possible charge modulations at multiples of the $\mathbf{Q}$, the conduction electron spin $\boldsymbol{\sigma}$ is subject to the exchange coupling $\boldsymbol{\Delta}(\mathbf{r}) \cdot \boldsymbol{\sigma}$, changing sign upon translation $\mathbf{T_b}$ by a single lattice spacing along the y axis, or by $2N$ spacings along the x axis: $\boldsymbol{\Delta}(\mathbf{r} + \mathbf{b}) = -\boldsymbol{\Delta}(\mathbf{r})$. Hence, in a transverse magnetic field, $\theta \mathbf{T_b} \mathbf{U_n}(\pi)$ is an antiunitary symmetry of the Hamiltonian, where θ is time reversal, and $\mathbf{U_n}(\pi)$ is a spin rotation by π around the unit vector $\mathbf{n}$ of the staggered magnetization. Retracing the derivation of Eq. (5) in Ref. [17], one finds

$$\langle \mathbf{p}|\theta \mathbf{T_b} \mathbf{U_n}(\pi)|\mathbf{p}\rangle = e^{-2i\mathbf{p}\cdot\mathbf{b}} \langle \mathbf{p}|\theta \mathbf{T_b} \mathbf{U_n}(\pi)|\mathbf{p}\rangle. \quad (4)$$

Thus, a Bloch eigenstate $|\mathbf{p}\rangle$ at a momentum $\mathbf{p}$ is orthogonal to its partner $\theta \mathbf{T_b} \mathbf{U_n}(\pi)|\mathbf{p}\rangle$ at the momentum $-\mathbf{p}$ [23]. In the folded Brillouin zone, defined by the periodicity of the $\boldsymbol{\Delta}(\mathbf{r})$, the momenta $\mathbf{p}^* = (\frac{\pi}{2Na}[2k + 1], \frac{\pi}{2a})$ and $-\mathbf{p}^*$ are equivalent for an integer k. Hence, Eq. (4) proves the Kramers degeneracy of the Bloch eigenstates at $\mathbf{p} = \mathbf{p}^*$ in a transverse magnetic field. In two dimensions, the equation $g_\perp(\mathbf{p}) = 0$ defines a line in the Brillouin zone, and Eq. (4) pins this line at the above symmetry-enforced degeneracy points S, as shown in Fig. 2(a) for $\mathbf{Q} = (\frac{3\pi}{4a}, \frac{\pi}{a})$.

The S points do tend to host a band extremum [9,10]. The leading term of the momentum expansion of the $g_\perp(\mathbf{p})$ around these points is linear, and the Landau levels and their Zeeman splitting have been described in Refs. [12–14]. A carrier pocket may also be centered at a point, where the line $g_\perp(\mathbf{p}) = 0$ intersects itself, as it does at the point X in Fig. 2(b). The leading term of the momentum expansion of the $g_\perp(\mathbf{p})$ around the point X is quadratic [14,17], and the carrier Hamiltonian near the point X takes the form

$$\mathcal{H} = \frac{\mathbf{p}^2}{2m} - (\boldsymbol{\Omega}_\parallel \cdot \boldsymbol{\sigma}) - \frac{p_x^2 - p_y^2}{2m\Delta}(\boldsymbol{\Omega}_\perp \cdot \boldsymbol{\sigma}), \quad (5)$$

where $\boldsymbol{\Omega} \equiv \frac{1}{2} g_\parallel \mu_B \mathbf{H}$. The small pocket size implies that $\frac{p_F^2}{m\Delta} \sim \frac{\mu}{\Delta} \ll 1$, where μ is the chemical potential, counted from the bottom of the pocket.

According to the Hamiltonian (5), in a transverse field ($\boldsymbol{\Omega}_\parallel = 0$) the Landau levels undergo no Zeeman splitting, while the effective mass tensor becomes anisotropic and dependent on the spin projection onto $\boldsymbol{\Omega}_\perp$ as per $m_{x/y}^{-1} = m^{-1}[1 \pm \frac{(\boldsymbol{\Omega}_\perp \cdot \boldsymbol{\sigma})}{\Delta}]$, as shown in Fig. 3. Beyond the spin-flop threshold, the staggered magnetization reorients itself transversely to the field; thus, the Landau levels undergo no Zeeman splitting, and no spin zeros are to be found in any field direction.

Near the spin flop but with $\boldsymbol{\Omega}_\parallel \neq 0$ in the Hamiltonian (5), the Zeeman splitting $\delta\mathcal{E}$ of the Landau levels is simply $\delta\mathcal{E} = 2\Omega_\parallel$ [14], with small corrections of the order of $[\mu/\Delta]^2 \ll 1$: at a low enough doping, $\delta\mathcal{E}$ behaves as if the last term in Eq. (5) simply vanished.

Hence, according to Eq. (1), for a small pocket at the point X, the field direction of the lth spin zero in the main harmonic ($k = 1$) satisfies the equation

$$\frac{\delta\mathcal{E}}{\Omega_0} = \eta \frac{H_\parallel}{H_0} = \eta \tan\theta \cos\varphi = l + \frac{1}{2}, \quad (6)$$

where $\eta = g_\parallel \mu_B \frac{mc}{\hbar e} = \frac{g_\parallel}{2} \frac{m}{m_0}$, l is an integer, $H_0 = H\cos\theta$ is defined in Fig. 1, and $H_\parallel = H \sin\theta \cos\varphi$ is the longitudinal component of the field with respect to the staggered magnetization.

The distinction between the above spin zeros and those of the S and Σ pockets stems from the leading term of the momentum expansion of the $g_\perp(\mathbf{p})$ around the points S and Σ being linear rather than quadratic:

$$\mathcal{H} = \frac{p_x^2}{2m_x} + \frac{p_y^2}{2m_y} - (\boldsymbol{\Omega}_\parallel \cdot \boldsymbol{\sigma}) - \frac{\xi p_y}{\hbar}(\boldsymbol{\Omega}_\perp \cdot \boldsymbol{\sigma}), \quad (7)$$

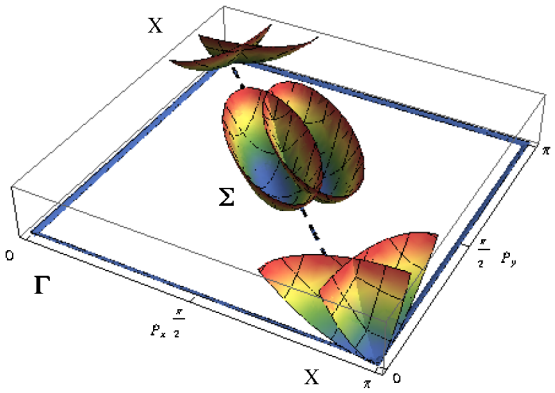

FIG. 3 (color online). A sketch of the Zeeman splitting of the small carrier pockets, centered at the points $X = (0, \frac{\pi}{a})$ [Eq. (5)] and $\Sigma = (\frac{\pi}{2a}, \frac{\pi}{2a})$ [Eq. (7)] in the first quadrant of the Brillouin zone, in a purely transverse magnetic field. The dashed line, passing through the points X and Σ, is the magnetic Brillouin zone boundary, where $g_\perp(\mathbf{p}) = 0$. The pocket sizes and the splitting are greatly exaggerated.

where p_y is the transverse component of the momentum with respect to the magnetic Brillouin zone boundary in Fig. 3. Here, as at the point X, the carrier pocket is assumed small enough to be described by Eq. (7): $\frac{\xi p_y}{\hbar} \lesssim \sqrt{\frac{\mu}{\epsilon^*}} \ll 1$, where $\epsilon^* = \frac{\hbar^2}{2m_y\xi^2} \sim \frac{\Delta^2}{\epsilon_F}$, and μ is the chemical potential, counted from the bottom of the pocket. The length scale ξ is of the order of the antiferromagnetic coherence length $\hbar v_F/\Delta$ [17]. The spin zeros for such a pocket, encapsulated in Eq. (11) of Ref. [12], differ from those given by Eq. (6) only via the small parameter $\sqrt{\frac{\mu}{\epsilon^*}} \ll 1$. This quantitative and, for most field orientations, numerically small difference is likely to render experimentally distinguishing the Σ pockets from their X counterparts rather difficult, especially on the background of the Fermi surface corrugation [24] and bilayer splitting [7]. These effects also modify the oscillation amplitude in a material-specific way [7,24].

To conclude, I have shown that, in an antiferromagnet, a combination of symmetry arguments with the knowledge of the possible positions of the band extrema [25] allows us to either constrain the possible locations of a small carrier pocket, or even to pinpoint it in the Brillouin zone by mapping the spin zeros of the quantum oscillation amplitude. This opportunity arises due to the anisotropic spin-orbit character of the Zeeman coupling in an antiferromagnet, and does not exist in a paramagnetic conductor. While I use the $\mathbf{Q} = (\frac{\pi}{a}[1 - \frac{1}{2N}], \frac{\pi}{a})$ and $\mathbf{Q} = (\frac{\pi}{a}, \frac{\pi}{a})$ spin density waves as an illustration, possibly relevant to cuprate superconductors, the method is applicable to many other antiferromagnets, such as iron pnictides, and organic and heavy fermion materials.

I am grateful to the Condensed Matter Theory groups of the ICTP in Trieste and MPI PKS in Dresden, where parts of this work were done, for kind hospitality. I thank C. Capan, B. Vignolle, D. Vignolles, and especially C. Proust for helpful comments, and M. R. Norman and A. J. Millis for extended discussions.

[1] D. Shoenberg, *Magnetic Oscillations in Metals* (Cambridge University Press, Cambridge, England, 1984).
[2] N. Doiron-Leyraud, C. Proust, D. LeBoeuf, J. Levallois, J.-B. Bonnemaison, R. Liang, D. A. Bonn, W. N. Hardy, and L. Taillefer, Nature (London) **447**, 565 (2007).
[3] E. A. Yelland, J. Singleton, C. H. Mielke, N. Harrison, F. F. Balakirev, B. Dabrowski, and J. R. Cooper, Phys. Rev. Lett. **100**, 047003 (2008).
[4] A. F. Bangura, J. D. Fletcher, A. Carrington, J. Levallois, M. Nardone, B. Vignolle, P. J. Heard, N. Doiron-Leyraud, D. LeBoeuf, L. Taillefer, S. Adachi, C. Proust, and N. E. Hussey, Phys. Rev. Lett. **100**, 047004 (2008).
[5] C. Jaudet, D. Vignolles, A. Audouard, J. Levallois, D. LeBoeuf, N. Doiron-Leyraud, B. Vignolle, M. Nardone, A. Zitouni, R. Liang, D. A. Bonn, W. N. Hardy, L. Taillefer, and C. Proust, Phys. Rev. Lett. **100**, 187005 (2008).
[6] S. E. Sebastian, N. Harrison, E. Palm, T. P. Murphy, C. H. Mielke, R. Liang, D. A. Bonn, W. N. Hardy, and G. G. Lonzarich, Nature (London) **454**, 200 (2008).
[7] A. Audouard, C. Jaudet, D. Vignolles, R. Liang, D. A. Bonn, W. N. Hardy, L. Taillefer, and C. Proust, Phys. Rev. Lett. **103**, 157003 (2009).
[8] A. Carrington and E. A. Yelland, Phys. Rev. B **76**, 140508 (R) (2007); I. S. Elfimov, G. A. Sawatzky, and A. Damascelli, Phys. Rev. B **77**, 060504(R) (2008).
[9] A. J. Millis and M. R. Norman, Phys. Rev. B **76**, 220503 (R) (2007).
[10] N. Harrison, Phys. Rev. Lett. **102**, 206405 (2009).
[11] W.-Q. Chen, K.-Y. Yang, T. M. Rice, and F. C. Zhang, Europhys. Lett. **82**, 17004 (2008).
[12] V. V. Kabanov and A. S. Alexandrov, Phys. Rev. B **77**, 132403 (2008); **81**, 099907(E) (2010).
[13] R. Ramazashvili, Phys. Rev. B **80**, 054405 (2009).
[14] R. Ramazashvili, Zh. Eksp. Teor. Fiz. **100**, 915 (1991) [Sov. Phys. JETP **73**, 505 (1991)].
[15] S. A. Brazovskii and I. A. Luk'yanchuk, Zh. Eksp. Teor. Fiz. **96**, 2088 (1989) [Sov. Phys. JETP **69**, 1180 (1989)].
[16] R. Ramazashvili, Phys. Rev. Lett. **101**, 137202 (2008).
[17] R. Ramazashvili, Phys. Rev. B **79**, 184432 (2009).
[18] D. Haug, V. Hinkov, A. Suchaneck, D. S. Inosov, N. B. Christensen, Ch. Niedermayer, P. Bourges, Y. Sidis, J. T. Park, A. Ivanov, C. T. Lin, J. Mesot, and B. Keimer, Phys. Rev. Lett. **103**, 017001 (2009).
[19] D. LeBoeuf, N. Doiron-Leyraud, R. Daou, J.-B. Bonnemaison, J. Levallois, N. E. Hussey, C. Proust, L. Balicas, B. Ramshaw, R. Liang, D. A. Bonn, W. N. Hardy, S. Adachi, and L. Taillefer, Nature (London) **450**, 533 (2007).
[20] M. R. Norman and Jie Lin, Phys. Rev. B **82**, 060509(R) (2010).
[21] Suchitra E. Sebastian, N. Harrison, C. H. Mielke, Ruixing Liang, D. A. Bonn, W. N. Hardy, and G. G. Lonzarich, Phys. Rev. Lett. **103**, 256405 (2009).
[22] B. J. Ramshaw, B. Vignolle, J. Day, R. Liang, W. N. Hardy, C. Proust, and D. A. Bonn, arXiv:1004.0260.
[23] On the lines $p_x = k\frac{\pi}{a}$ and $p_y = k\frac{\pi}{Na}$ with $k = 0, \pm 1, \pm 2, \ldots$, the exponent on the right-hand side of Eq. (4) equals unity, and the degeneracy is not protected.
[24] N. Harrison and R. D. McDonald, J. Phys. Condens. Matter **21**, 192201 (2009).
[25] The band extrema tend to fall at the high-symmetry points in the Brillouin zone, and are readily identified by relatively simple calculations such as those cited above.